

A LABORATORY STUDY FOR DUAL-POLARIZATION SCATTERING CHARACTERISTICS OF METEOROLOGICAL OBJECTS

Andrew Huston, Yan Zhang*, Guifu Zhang, Mark Yeary
University of Oklahoma, Norman, OK 73072

KEYWORDS **Dual-polarization, Scattering, Hydrometeors, Scatterometer**

1. INTRODUCTION

The radar sensors with dual-polarization capability allow better understanding and characterization of weather hazards. Advanced knowledge-based hazard detection algorithms would require better knowledge of wave scattering characteristics of hydrometeors such as raindrops, hailstones, and snowflakes. Especially, scattering characteristics becomes important for optimally utilize phase-array dual-polarization radar systems. Traditionally, theoretical approaches [1] have been used to calculate the scattering characteristics while controlled lab-measurements have not been fully explored. In this abstract, an experimental approach is adopted with the assistance of a controlled laboratory environment. The advanced Agilent PNA network analyzer-based scatterometer system design is introduced. The key Radar Cross-Section (RCS) parameters and preliminary validation through actual scattering measurements are discussed.

It is expected that the calibrated scatterometer system can be used to characterize emulated or natural weather hazard samples. While it is known that the actual meteorological targets are generally considered as random and distributed targets consisting of a large volume of point scatterers, and the volume scattering field can be viewed as the superposition of all the point scatterers in the radar resolution volume, as a first-order solution of N-particle scattering problem [2]:

$$\mathbf{F}^{(1)}(\bar{\mathbf{k}}_s, \bar{\mathbf{k}}_i) = \sum_{p=1}^N f_p \exp(j\bar{\mathbf{k}}_d \cdot \bar{\mathbf{r}}_p), \quad (1)$$

where \mathbf{F} is the total scattering amplitude of the \mathbf{E} field, f_p is the scattering coefficient of the pth particle, $\bar{\mathbf{k}}_s$ and $\bar{\mathbf{k}}_i$ are the direction vector for scattering and incidental wave, respectively, $\bar{\mathbf{k}}_d = \bar{\mathbf{k}}_i - \bar{\mathbf{k}}_s$ and $\bar{\mathbf{r}}_p$ is the position vector of the pth scatterer. From (1), it is important to understand the scattering properties for each individual scatterer before extending to the entire volume scattering situation. This approach requires the

knowledge of amplitude, phase and frequency variation of the bi-static scattering for a single scatterer. The lab measurement can be combined with simulation prediction to validate this knowledge.

In addition to traditional theoretical tools, a fast method to simulate dual-polarized RCS for single or small number of scatterers with arbitrary shape/orientation is using commercial EM solvers (such as HFSS®), and then a Monte-Carlo simulation can be run to predict the volume scattering of a large number of identical scatterers. The simulation results can then be compared with lab measurement for verification. Because of the sensitivity limitation of the scatterometer system, the simulation data should be combined with lab measurement as a preferable source about the knowledge of very small particles.

2. THE SYSTEM SETUP AND CALIBRATION

A PNA E8364B network analyzer is being used as a centerpiece for performing various in-door measurements. The PNA system is powerful equipment from Agilent which simplifies the traditional antenna and RCS measurement process. This multi-function scatterometer, which can cover from S-band to Ku-band (3-18 GHz) with a simple system configuration, can emulate continuous wave transmit signal at different frequencies as well as the pulsed waveform of a phased-array radar. The conceptual scatterometer configuration is set up as shown in Figure 1. Thus far, the internal gating contained in the PNA network analyzer has been sufficient so that no external gating hardware has been required. The dimensions of the range are such that far-field requirements are met and the height of the antennas from the ground is sufficient to control ground reflection and sidelobe interference. The scatterometer has the parameters listed in Table 1, which make it well suited for the in-door RCS characterizations.

Table 1: System parameters of the scatterometer

Frequency coverage	S-Ku band (3-18 GHz)
Centerpiece	Agilent E8364B network analyzer
Transmit power	20 dBm
Antenna	Dual-polarized horn and low-sidelobe range illumination horns

*Corresponding author: Yan Zhang, School of Electrical and Computer Engineering, University of Oklahoma, Norman OK 73072, Email: rockee@ou.edu

Polarization	Able to conduct simultaneous polarization measurement with appropriate antenna configuration
Sensitivity	Better than -110 dBm at 6-12 GHz frequency band
Measurement control	PC and Ethernet
Waveform	Continuous or pulsed

The chamber itself has been lined with standard radar-absorbing foam along all significant surfaces. This and other modifications have resulted in a transmit-to-receive power ratio of -90 dB in the frequency domain and -110dB in the time domain for the empty range. A rig has been specially designed to allow the suspension of different-sized targets using a low ϵ_r net constructed of monofilament. The rig allows the target to be stably suspended and allows the height of the target to be adjusted from behind the antennas without needing to go downrange.

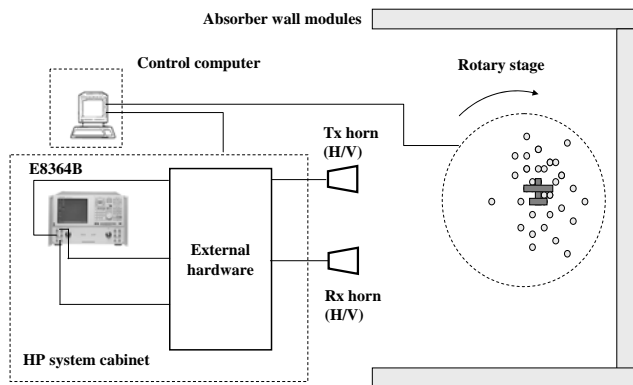


Figure 1 Scatterometer system setup

For a single scatterer, the dual-polarized RCS is measured from radar range equation:

$$\frac{P_{r(h,v)}}{P_{t(h,v)}} = \frac{G_t G_r \lambda^2 \sigma_{(h,v)}}{(4\pi)^3 R^4}, \quad (2)$$

where P_r is the received signal power for multiple polarizations, P_t is the transmit signal power for multiple polarizations, λ is the wavelength, and R is the range of the target under test. G_t and G_r denote transmit and receive antenna gain, respectively, and vary with wavelength according to the antenna specifications. $\sigma_{(h,v)}$ is the multi-polarized RCS to be measured. From (2), RCS can be derived by measuring T-R power ratio at specific frequencies for a fixed-range target.

The scatterometer is calibrated with aluminum spheres with different diameters. A comparison of a scatterer's RCS measured from (2) to the theoretical results

obtained from Mie scattering theory approximation shows an excellent correlation as shown in Figure 2.

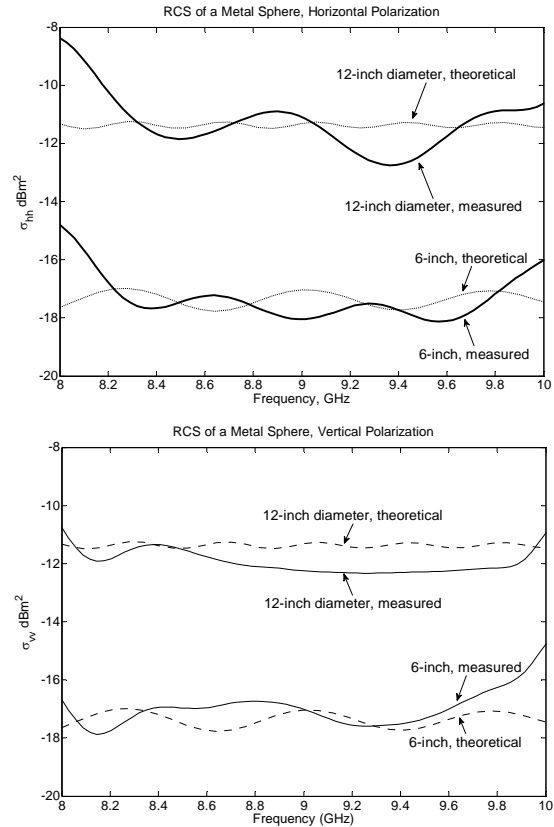


Figure 2 shows the dual-polarized RCS measurement for 6- and 12-inch diameter calibration balls (made by aluminum) at X-band (8-10 GHz). The measurement results based on this chamber have close agreements with the theoretical predictions (dashed lines).

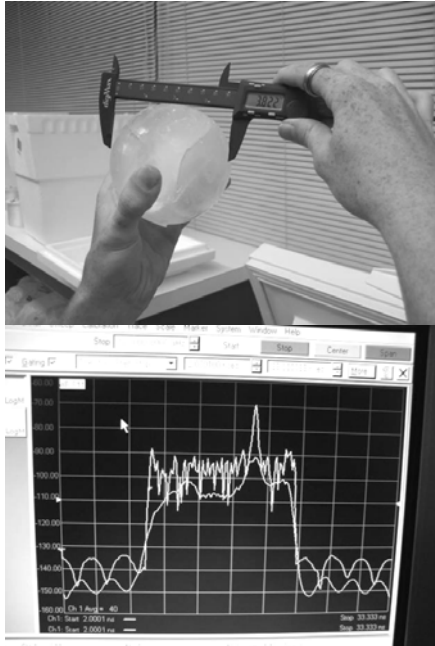
3. PRELIMINARY MEASUREMENT RESULTS OF SOME EMULATED METEOROLOGICAL TARGETS

At this time, our current lab-measurement effort focuses on the frequency variation of the dual-polarized monostatic RCS for small number of meteorological scatterers. Also, we focused on comparing the dual-polarized RCS of emulated meteorological targets with a perfect conductor sphere at X-band. The scattering phase measurement and large-volume scattering results will be reported later as experimental data and theoretical models are developed.

3.1 Large emulated ice balls

Measurement results with a 3.6" diameter man-made 'super hailstone' are shown in Figure 3-4. Spheres were constructed of uniform ice as well as layered ice of differing densities. This was accomplished by using ice

from different sources frozen in succession. The large size of the spheres permitted strong measurements with radar and gave information that can be applied to smaller particles less easy to individually measure. Initial measurements show a difference in σ_{hh} and σ_{vv} for the ice balls, as well as greater fluctuation across the frequency range. The discrepancy in vertical to horizontal RCS response can also be observed in theoretical predictions at 10 GHz. This can prove useful in identifying and classifying specific hydrometeors.



(a) A man-made 'super hail' (before melting to 3.6" diameter)
 (b) The time-domain range profile of the man-made 'super-hail' (6 - 12 GHz frequency band)

Figure 3: Measurement of the polarimetric RCS for a single man-made 'super hail'. Time-domain transformation and gating of the PNA are used to suppress noise, T-R coupling and interference.

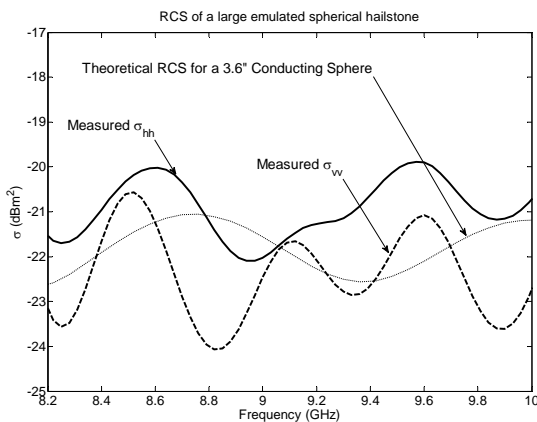


Figure 4: Measured dual-polarized RCS of the man-made hail and comparison to theoretical prediction of RCS of a

perfect metal sphere with the same diameter. It is seen that the two polarizations have much stronger differences in two polarizations and more frequency variations are observed.

3.2 Iced-filled ping-pong ball

As a more realistic emulation of the natural hail storm (particularly in size of the hail), ice-filled ping-pong balls (1.5" diameter) are measured using the scatterometer system. A single ice-filled ping-pong ball yields ~10 dB signal-to-noise ratio at 2.0-meter (far field) measurement distance. A typical measurement result is shown in Figure 5. Again, a difference in the vertical and horizontal RCS is observed.

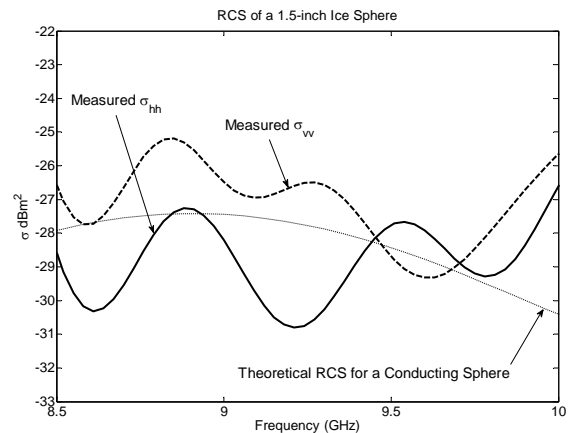


Figure 5: Measured dual-polarized RCS of an ice-filled ping-pong ball and comparison to theoretical prediction of RCS of a perfect metal sphere with the same diameter.

3.3 Small scale clustered/volume scatterers

The next step in the experiment is to create a volume distribution of ice spheres. This work is still in progress while some simple volume-scattering tests by fast measuring clusters of 1.5-inch ice spheres has been performed. The ice-spheres are suspended in a net made with low- ϵ_r monofilament and agitated to emulate random motion and distribution. 60 points of RCS data samples are obtained and averaged from 9 to 9.5 GHz frequency range. As we can see from the example in Figure 7, the σ_{VV} measurement shows a slight increase of RCS from single sphere to a stack of 3 spheres, while a larger increase in RCS is observed for stacks of 4 and 5 spheres. The figure also illustrates the importance of phase information when characterizing hydrometeors. The phase of the backscattered radiation is dependent on the size of the cluster, and so can give information regarding the makeup of a volume distribution of ice spheres.

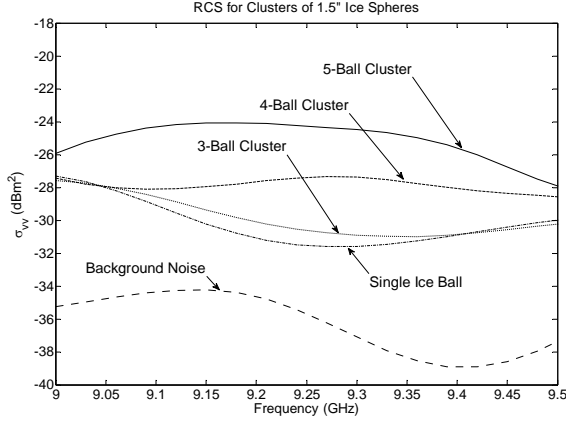


Figure 6: Example measurement results of σ_{VV} , which compares the RCS of background noise, a single ice sphere, 3-ball, 4-ball and 5-ball clusters.

4. EXPLOITING THE PHASE INFORMATION OF SCATTERING FIELDS

For more advanced distributed target characterization and hazard classification, the complex (bi-static) RCS [4] $\sqrt{\sigma}$ is also a key parameter for the polarimetric scattering characterization. In HFSS, the complex RCS is defined as

$$\sqrt{\sigma} = 2\sqrt{\pi R} \frac{\mathbf{E}_{\text{scattered}, \phi \text{ or } \theta}}{|\mathbf{E}_{\text{incident}}|}, \quad (3)$$

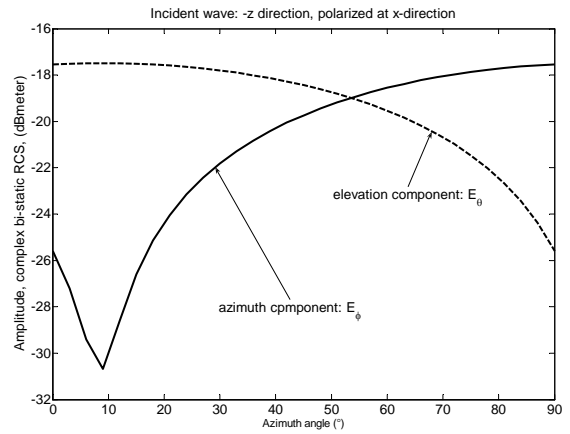
As an example, Figure 7 shows a typical bi-static RCS (amplitude and phase) for a single ice-spheroid as a result of different incident wave polarization at $\theta = 0^\circ$ (backscattering) and different azimuth angles. Polarimetric radar signatures can be derived based on such data and can be used for further weather hazard characterizations. The reason that $\sqrt{\sigma}$ will be important for our future applications is when the PNA network analyzer and a rotary positioner is used, the amplitude and phase of $\sqrt{\sigma}$ can be directly measured based on vector-S-parameter concepts. Taking into account the phase of $\sqrt{\sigma}$ will allow further differentiation of different type of hydrometers or weather hazards.

5. CONCLUSION

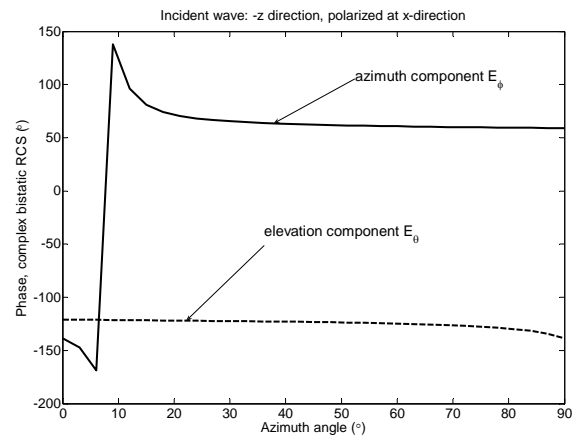
A controlled lab-measurement approach is introduced to characterize dual-polarization scattering characteristics of hydrometeor hazards. An advanced network analyzer instrument is used as the centerpiece of the scatterometer measurement system. Preliminary results show that the lab-measurements agree well with theoretical calculations and the potential target discrimination capabilities. More realistic meteorological targets will be modeled for the experiments and calculation in future.

REFERENCES

- [1] J. Vivekanandan, R. Raghavan, and V.N. Bringi, "Polarimetric Radar Modeling of Mixtures of Precipitation Particles", *IEEE Trans. on Geoscience and Remote Sensing*, vol. 31(5), pp. 1017-1030, 1993.
- [2] L. Tsang, J.A. Kong, K-H. Ding and C.O. Ao, *Scattering of Electromagnetic Waves: Numeric Simulations*, John Wiley & Sons, Inc., 2001.
- [3] T. Oguchi, S. Ishii, S. Ito, and T.Manabe, "Laboratory measurements of radar depolarization signatures in microwave pulse transmission through randomly distributed spherical scatterers", *IEEE Trans. on Geoscience and Remote Sensing*, vol. 36(3), pp. 1011-1015, 1998.
- [4] S. Riegger and W. Wiesbeck, "Wide-band Polarimetry and Complex Radar Cross Section Signatures", *Proceedings of the IEEE*, vol.77 (5), pp. 649-658, 1989.



(a) The amplitude vs. elevation angle



(b) The phase vs. elevation angle

Figure 7 Bi-static complex RCS amplitude and phase for a simulated ice spheroid, the main axis is X-axis (30 mm length) and axis ratio is 0.2. The incident wave is x-polarized, the solid line is for ϕ -component complex RCS and the dashed line is for θ -component complex RCS. The scattering field is computed from HFSS®.